A competition-attenuation mechanism modulates thermoresponsive growth at warm temperatures in Arabidopsis

Wei Li[1,2], Ying-Ying Tian[1], Jin-Yu Li[1], Li Yuan[3], Lin-Lin Zhang[1], Zhi-Ye Wang[1], Xiaodong Xu[3], Seth Jon Davis[3,4] and Jian-Xiang Liu [1, *]

[1]State Key Laboratory of Plant Physiology and Biochemistry, College of Life Sciences, Zhejiang University, Hangzhou 310027, China.

[2]College of Environmental and Resource Sciences, Zhejiang University, Hangzhou 310027, China.

[3]State Key Laboratory of Crop Stress Adaptation and Improvement, School of Life Sciences, Henan University, Kaifeng 475004, China.

[4]Department of Biology, University of York, Heslington, York, YO105DD, UK.

[*]Correspondence：jianxiangliu@zju.edu.cn

Article type:

Research article

Short title:

RVE5 regulates thermoresponsive growth

Plain Language Summary:

Warm-temperature induced REVEILLE 5 (RVE5) impedes hypocotyl growth through competing with CCA1 in joint repression tuning of *ELF4*-induced inhibition of thermo-responsive growth in Arabidopsis.

Summary

- Global warming has profound impact on growth and development, and plants constantly adjust their internal circadian clock to cope with external environment. However, how clock-associated genes fine-tune thermoresponsive growth in plants is still less understood.
- We found that loss-of-function mutation of *REVEILLE5* (*RVE5*) reduces the expression of circadian gene *EARLY FLOWERING 4* (*ELF4*) in *Arabidopsis*, and confers accelerated hypocotyl growth under warm-temperature conditions.
- Both RVE5 and CIRCADIAN CLOCK ASSOCIATED 1 (CCA1) accumulate at warm temperatures and bind to the same EE *cis*-element presented on *ELF4* promoter, but the transcriptional repression activity of RVE5 is weaker than that of CCA1.
- The binding of CCA1 to *ELF4* promoter is enhanced in the *rve5-2* mutant at warm temperatures, and overexpression of *ELF4* in the *rve5-2* mutant background suppresses the *rve5-2* mutant phenotype at warm temperatures.
- Therefore, the transcriptional repressor RVE5 finetunes *ELF4* expression via competing at a cis-element with the stronger transcriptional repressor CCA1 at warm temperatures. Such a competition-attenuation mechanism provides a balancing system for modulating the level of ELF4 and thermoresponsive hypocotyl growth under warm temperature conditions.

Keywords: *Arabidopsis thaliana*, Hypocotyl growth, Thermomorphogenesis, Warm temperature

Introduction

Plants have evolved an internal timing keeping-mechanism known as the circadian clock that enables anticipation of external environmental cues to adjust growth and development (Huang & Nusinow, 2016). This clock consists of the input and output pathways, and the central oscillator (Creux & Harmer, 2019). Ambient light and temperature cues are two major inputting signals that function at both transcriptional and post-translational levels to set (entrain) this clock (Hsu & Harmer, 2014). The central oscillator at ambient temperature contains multiple repressors and activators that form interconnected feedback loops. Briefly, the morning expressed CCA1 and LATE ELONGATED HYPOCOTYL (LHY) repress the expression of afternoon genes *PSEUDO-RESPONSE REGULATOR1* (*PRR1*/*TIMING OF CAB EXPRESSION1* (*TOC1*), *PRR5*, *PRR7*, and *PRR9;* in turn, the latter encoded proteins inhibit the expression of former genes *CCA1*/*LHY* (Alabadi *et al.*, 2001; Kamioka *et al.*, 2016). CCA1/LHY also inhibit the expression of evening genes of the Evening Complex (EC); and EC represses the expression of PRRs (Herrero *et al.*, 2012; Mizuno *et al.*, 2014). In addition, midday-expressed REVEILLE 4/6/8 (RVE4/6/8) activate the expression of *TOC1*, PRR5, and EC genes, but *RVE8* expression is inhibited by TOC1 and other PRRs (Rawat *et al.*, 2011; Hsu *et al.*, 2013; Hsu & Harmer, 2014). Further, GIGANTEA (GI) promotes the expression of *CCA1*/*LHY* whereas CCA1/LHY inhibits the expression of *GI* and *TOC1* (Fowler *et al.*, 1999; Mizoguchi *et al.*, 2002). These multiple feedback loops provide rhythmic robustness across dynamic environmental conditions (Shalit-Kaneh *et al.*, 2018). As output pathways, the circadian clock regulates diurnal hypocotyl growth and photoperiod-dependent flowering (Farre, 2012).

Global warming has world-wide impacts on plant distribution and crop productivity (Lesk *et al.*, 2016). The plant circadian clock also controls hypocotyl growth under warm-temperature conditions, in a process termed

thermomorphogenesis, in which plants sense and adapt to ambient warm temperatures (Park *et al.*, 2021). Several proteins/RNAs have been proposed to be warm temperature sensors in plants. For example, phytochrome B (phyB), originally characterized as a photoreceptor (Lin *et al.*, 2020), is a temperature sensor. Warm temperature accelerates the conversion of phyB from active Pfr to inactive Pr, which reduces the inhibitory effects of phyB on a bHLH transcription factor phytochrome interacting factor 4 (PIF4) (Jung *et al.*, 2016; Legris *et al.*, 2016). PIF4 is the central regulator of plant thermomorphogenesis and subjected to multiple regulation both at transcriptional and post-translational levels (Vu *et al.*, 2019). It recognizes G-box (CACGTG)-containing *cis*-elements and regulates the expression of downstream genes involved in auxin biosynthesis and signaling (Franklin *et al.*, 2011; Sun *et al.*, 2012).

EARLY FLOWERING3 (ELF3) is another proposed temperature sensor, which undergoes liquid-liquid phase separation at warm temperatures (Jung *et al.*, 2020). It is a core component of the circadian clock and assembles into EC together with ELF4 and LUX ARRHYTHMO (LUX) (Thines & Harmon, 2010; Nusinow *et al.*, 2011; Huang & Nusinow, 2016). ELF4 binding to ELF3 recruits to a nuclear structure {Herrero, 2012 #7;Kolmos, 2011 #58} associated to activity {Anwer, 2014 #63;Ronald, 2022 #64;Ronald, 2021 #62}. Allelic variation within ELF3 has revealed that the presence of these nuclear foci correlates with both circadian function {Anwer, 2014 #63} and thermomorphogenesis {Raschke, 2015 #61}. Indeed, under warm conditions ELF3 disassociates from these active form {Ronald, 2021 #62}, as do phyB signals {Kolmos, 2011 #58;Ronald, 2022 #64}.

EC binds to the promoter of *PIF4*/*5* to inhibit gene expression, and such inhibition is reduced under warm temperature conditions (Nomoto *et al.*, 2012; Box *et al.*, 2015; Jung *et al.*, 2020; Silva *et al.*, 2020). Further, the EC plays a major role in directly coordinating the expression of hundreds of key regulators

of photosynthesis, the circadian clock, phytohormone signaling, growth and response to the environment (Ezer *et al.*, 2017). In addition, ELF3 also interacts with PIF4 protein and suppresses the transcriptional activity of PIF4 in an EC-independent manner (Nieto *et al.*, 2015). Under warm temperature conditions, ELF3 is subjected to ubiquitination-mediated protein degradation (Ding *et al.*, 2018; Zhang *et al.*, 2021a; Zhang *et al.*, 2021c). LUX is a strong DNA-binding MYB transcription factor while the LUX-ELF3 complex is a relatively poor binder of DNA, but its binding activity is much enhanced by adding ELF4 to the complex during *in vitro* assays (Silva *et al.*, 2020). This has been interpreted as that ELF4 acts a modulator of thermomorphogenesis. Indeed, ELF4 protein moves from shoots to regulate rhythms in roots in a temperature-dependent manner (Chen *et al.*, 2020). However, how the ELF4 activity is regulated in plants during thermomorphogenesis is less understood. Relevance here is that increased ELF4 levels generates more ELF3 activity {Herrero, 2012 #60;Kolmos, 2009 #47;McWatters, 2007 #65}. We thus hypothesized that a component of thermomorphogenesis would be regulation of ELF4 levels.

In this paper, we report the essential role of RVE5 in inhibiting hypocotyl growth at warm temperatures in *Arabidopsis*. We demonstrate that the transcriptional repressor RVE5 maintains *ELF4* expression at warm temperatures via competing with another transcriptional repressor CCA1, in which both RVE5 and CCA1 bind to the same *cis*-element presented on the *ELF4* promoter. As RVE5 has a weaker transcription repression activity relative to that of CCA1, the *rve5* mutant thus has more CCA1 activity leading to increased growth in warmth.

Materials and methods

Plant materials and hypocotyl length measurements

The *rve5-2* T-DNA mutant (GK_225C06) was obtained from the Nottingham *Arabidopsis* Stock Centre (NASC). *pif4-101* was previously described (Ding *et*

al., 2018). For the genetic complementation experiment, genomic sequences of *RVE5* including 1.8 kb upstream promoter sequences were amplified and subcloned into pCambia1300, and introduced to the *rve5-2* mutant background via an Agrobacterium-mediated floral dip method (Clough & Bent, 1998). For *RVE5* overexpression, the coding region (CDS) of *RVE5* cDNA was amplified and subcloned into pSKM36 and introduced to the wild-type (WT) background to express *RVE5-MYC* driven by the 35S promoter. For *CCA1-FLAG* expression, the promoter (1.6 kb) sequences and CDS sequence of *CCA1* were amplified and subcloned into pCambia1300 in which the *FLAG* sequence was previously inserted, respectively, and the vector was introduced to the WT and *rve5-2* mutant background to produce the CCA1-FLAG fusion protein, respectively. For *ELF4* overexpression, the promoter (0.9 kb) sequence of HSP70 (AT3G12580) and CDS sequence of *ELF4* were amplified and subcloned into pCambia1300, respectively, and the vector was introduced to the WT and *rve5-2* mutant background, respectively. All the primers used to generate these constructions are provided in Table S1.

Seeds were surface sterilized with 50% ethanol for 1 min and then with 0.01% sodium hypochlorite solutions for 25 min, and subsequently washed with sterilized water for four times. All the seeds were sown directly on half-strength Murashige and Skoog (MS) medium (containing 1.2% sucrose and 0.6% agar, pH adjusted to 5.7), stratified at 4°C for 3 days, and then transferred to a standard plant incubator with the following settings: 22°C, white light 100 μmol/m^2/s, 16/8-hr day/night for 3 days, after which the plates were placed at 22°C or 29°C for 3-4 days, respectively. Plants were photographed and hypocotyl length was measured using ImageJ software (National Institutes of Health).

ChIP-Seq and ChIP-qPCR

ChIP assays were carried out following an integrated method with Chelex resin-based ChIP procedure and protein A agarose beads (Millipore, CA, USA) (Song *et al.*, 2015). Briefly, 14-day-old 35S:*RVE5-MYC/*CCA1*:CCA1-FLAG* overexpression plants were treated at 22°C or 29°C for the indicated time and sampled for fixation with 1% formaldehyde for 15 min, which was stopped by adding 0.15 M Glycine. After sonication in 0.8% SDS buffer, the mix was immunoprecipitated with *anti*-MYC antibody (Abmart), or *anti*-FLAG antibody (Abmart), or *anti*-GST (Abmart) as the IgG control. ChIP-Seq was performed with an illumina Novaseq™ 6000 (Genergy Bio, Shanghai, China), with details described previously (Gao *et al.*). Briefly, low quality and linker sequence fragments were removed and sequences less than 50 bp were filtered with Skewer. After that, unique mapping of high-quality reads to the reference genome was performed with Bowtie. Peak calling was performed with MACS and the binding peaks were obtained when comparing to that with the input sample ($P < 0.001$). The related genes with common binding peak region in the upstream 2 K in three replicates were considered as the targets of RVE5. The common binding *cis*-elements were identified using MEME. The specific and overlapping targets between RVE5 and CCA1 were shown in Venn diagram, and a hypergeometric probability test of overlapping degree was performed using R. The ChIP-Seq data is deposited in the Gene Expression Omnibus (GEO) under accession number GSE180381. ChIP-qPCR was performed with three biological replicates. All the primers used for ChIP-qPCR are listed in Table S1.

Electrophoretic Mobility Shift Assays (EMSA)

The CDS of *RVE5* and *CCA1* was subcloned into pETMAL-H to produce MBP-RVE5 and MBP-CCA1 recombinant proteins, respectively. The EE-element (5'-AAATATCT-3') derived from the *ELF4* promoter was synthesized and biotinylated with the Biotin 3'-end DNA Labelling Kit (Thermo Fisher Scientific).

A mutated EE form (5'-AAATCGAG-3') was used for the competition experiment. EMSA was performed using a LightShift Chemiluminescent EMSA Kit (Thermo Fisher Scientific), according to the manufacturer's protocols. Briefly, each binding reaction (20 mM HEPES, pH 7.2, 80 mM KCl, 0.1 mM EDTA, 10% glycerol, 2.5 mM DTT, 0.07 mg/ mL BSA, 8 ng/mL poly dI-dC) was set at room temperature for 20 min and run on a 5% non-denaturing polyacrylamide gel. After transferring to a nylon membrane (GE), the blot was UV light cross-linked, detected with the Chemiluminescent Nucleic Acid Detection Module (Thermo Fisher Scientific).

Luciferase assays and effector-reporter assays

For bioluminescence assay of the circadian rhythm, the promoter sequence of *CCR2* (1.3 kb) was amplified and inserted into pGreenII 0800, and then the fragment containing the promoter and firefly luciferase (LUC) gene sequences was subcloned into pCambia1300, which was introduced to the WT and *rve5-2* mutant background, respectively. For luciferase measurement, 5-day-old transgenic seedlings (17-19 plants) grown at 22°C (12 hr/12 hr day/night) were kept at 22°C or transferred to 29°C for one day, and then subjected to automatic luciferase measurement using a digital CCD camera for 4 days in continuous light after sprayed with 1 mM luciferin. Period was calculated by fast Fourier transform-nonlinear least squares (FFT-NLLS) provided by BRASS. Student's t-test was performed for statistical analysis. The experiments were performed for three times and similar results were obtained. For effector-reporter assays, sequences of the *ELF4* or *LexA* promoter were synthesized and inserted into pGreen0800-II with the 35S promoter included before the firefly luciferase gene to generate the reporter vector in which the renilla luciferase gene was driven by the 35S promoter. The coding sequence of LexA-RVE5 or LexA-CCA1 or RVE5 or CCA1 was inserted into the pCAMBIA1300-35S or pSKM36 vector to generate the effector vector. Different combination of constructs was transiently

expressed in tobacco (*Nicotiana benthamiana*) leaves via *Agrobacterium tumefaciens* strain GV3101. Three days after infiltration, luciferase activities were measured with a dual-luciferase reporter assay kit (Promega). All the primers are listed in Table S1.

RT-qPCR and western blotting analysis

For RT-qPCR, total RNAs were extracted with three biological replicates using an RNA Prep Pure Plant kit (Tiangen) and reverse transcribed using 5×PrimeScript RT Master Mix (Takara) and oligo (dT) primers. RT-qPCR was performed using SuperReal PreMix Color (Tiangen) in a CFX96 real-time system (Bio-Rad). ΔΔCt (threshold cycle) method was applied to calculate the gene expression. All the primers used are listed in Table S1. Western blotting was performed as described (Zhang *et al.*, 2021c). Total proteins were extracted with the extraction buffer (125 mM Tris-HCl, pH 8.0, 375 mM NaCl, 2.5 mM EDTA, 1% SDS and 1% β-mercaptoethanol). Afterward, proteins were separated in 4-20% SDS-PAGE gels and analyzed using *anti*-FLAG(Abmart), *anti*-MYC(Abmart), *anti*-tubulin (Abmart), respectively. Each immunoblot was quantified using ImageJ software.

Results

RVE5 inhibits thermoresponsive hypocotyl elongation in *Arabidopsis*

The RVE family proteins (RVE1 to RVE8) are morning-phased MYB-like transcription factors at ambient temperature that are homologous to the central clock genes CCA1 and LHY (Kuno *et al.*, 2003; Rawat *et al.*, 2009). In our previous study on transcriptomic analysis of heat stress responses in *Arabidopsis*, we found that *RVE5* was a lone RVE increased in expression by warming temperature (Zhang *et al.*, 2017). To explore if RVE5 is involved in warm temperature-mediated growth, we obtained a null mutant *rve5-2* with the T-DNA inserted in the first exon of *RVE5*, and the MYB DNA-binding domain of

RVE5 is predicted to be disrupted in the *rev5-2* mutant (Fig. S1a-b), and performed phenotypic analyses. We first checked the hypocotyl growth of WT and *rve5-2* mutant plants under both ambient (22°C) and warm (29°C) temperature conditions. The *rve5-2* mutant plants had a similar hypocotyl length as the WT plants at 22°C. In contrast, when compared with that of the WT, the hypocotyl length of *rve5-2* mutant was significantly taller at 29°C (Fig. 1a-b). The thermoresponsive hypocotyl phenotype of *rve5-2* mutant was rescued by introducing the genomic sequence of *RVE5* in three independent transgenic lines (Fig. 1a-b). This transgenic complementation confirms the important role of *RVE5* in plant thermomorphogenesis. We also generated 35S:*RVE5-MYC* overexpression plants (Fig. S2a-c). Consistent with RVE5 funstioning to suppress growth under warmth, the hypocotyl length of the overexpression plants (*RVE5ox*) was slightly shorter than that of the WT plants under warm temperature conditions (Fig. S2a-b). Although the expression of *RVE5* was found to be high in these transgenic plants (Fig. S2c), RVE5 protein accumulation may not have been sufficient for a stronger hypocotyl phenotype. We further checked the hypocotyl phenotype of *rve5-2* mutant and genetically complemented transgenic plants at both 22°C and 29°C in darkness, and the results showed that there were no obvious differences among these plant materials in terms of hypocotyl growth (Fig. S3), suggesting that the function of RVE5 in thermomorphogenesis is dependent on light. Thus, RVE5 is a negative regulator of thermomorphogenesis and essential for controlling hypocotyl growth at warm temperatures.

The bHLH transcription factor PIF4 is a central regulator of plant thermomorphogenesis (Koini *et al.*, 2009; Quint *et al.*, 2016). To analyze the genetic relationship between *RVE5* and *PIF4*, we generated the double mutant *rve5-2 pif4-101* and carried out epistatic analyses. Opposite to the *rve5-2* single mutant, but similar to the *pif4-101* single mutant, the hypocotyl of *rve5-2 pif4-*

278 *101* plants did not substantially elongate at 29°C (Fig. 1c-d). Thus, *PIF4* was
279 found to be epistatic to *RVE5* during thermomorphogenesis. Taken together,
280 these results support that *RVE5* functions upstream of *PIF4* in
281 thermomorphogenesis.

282 **RVE5 shares genome-wide direct targets with CCA1**

283 To next explore the mechanism of RVE5 in controlling thermoresponsive
284 growth, we performed biochemical analysis and Chromatin
285 Immunoprecipitation-Sequencing (ChIP-Seq). Firstly, we checked the protein
286 stability of RVE5 under warm temperature conditions with 35S:*RVE5-MYC*
287 overexpression plants (*RVE5*ox-4). Western blotting showed that the protein
288 level of RVE5-MYC was increased at 29°C comparing to that at 22°C (Fig. 2a).
289 Using these *RVE5-MYC* overexpression plants grown at 29°C, we performed
290 ChIP-Seq to examine chromatin occupancy of RVE5. The normalized IP signals
291 were peaked in the promoter regions (Fig. 2b), representing a typical
292 transcription factor binding characteristic. In total, 385 loci were identified that
293 are enriched in all of the three replicates (Table S2). Hereafter we refer them
294 as RVE5-targets. The *cis*-elements Evening Element (EE) responsible for
295 rhythmic gene expression (Nagel *et al.*, 2015) and G-box were highly enriched
296 in these binding peaks (Fig. 2c-d). Because RVE5 is a protein with sequence
297 similarity to CCA1, we compared RVE5 targets to previously identified CCA1
298 targets (Kamioka *et al.*, 2016). We found that RVE5 and CCA1 significantly
299 shared overlapping targets (P=3.6e-156) at 175 gene loci (Fig. 2e and Table
300 S2). Together, these results support that RVE5 shares some common direct
301 targets with CCA1.

302 **RVE5 binds to the promoter of clock-associated genes and regulates their**
303 **expression under warm temperature conditions**

304 The ChIP-Seq data revealed that RVE5 was enriched in the promoter regions
305 of many circadian clock genes, including *ELF4*, *LUX*, *TOC1*, *GI*, *PRR5*, *PRR7*,

306 and *CCR2* (Fig. 2f). However, RVE5 was hardly detected at the promoter of
307 *ELF3*, *CCA1*, *LHY1*, *PRR9* and *PIF4* (Fig. 2f). To check the effect of
308 temperature conditions on RVE5-binding to these direct targets, we selected
309 *ELF4*, *PRR5* and *PRR7*, and performed ChIP-qPCR to confirm and further
310 compare the RVE5-binding at both 22°C and 29°C. The results confirmed the
311 ChIP-Seq data and showed that warm temperature enhanced the binding of
312 RVE5 to the promoter of *ELF4*, *PRR5*, and *PRR7* (Fig. 2g-i).

313 To examine whether RVE5 regulates the timed expression of its target
314 clock genes, we carried out RT-qPCR to monitor gene expression at multiple
315 time points within two days under two different temperature conditions in the
316 WT and *rve5-2* mutant plants. The results showed that the expression of *ELF4*,
317 *CCA1*, *LHY1*, *PRR9*, *PRR7, PRR5*, *TOC1*, *GI*, and *CRR2* was affected in the
318 *rve5-2* mutant at 29°C at least at one timepoint when compared to that of the
319 WT plants, while the expression of *ELF3* and *LUX* was not appreciably affected
320 in the *rve5-2* mutant (Fig. 3). For example, there was no obvious difference in
321 the expression level of *ELF4* at 22°C between WT and *rve5-2* mutant, however,
322 the expression of *ELF4* was much lower in *rve5-2* mutant than that in WT plants
323 at 29°C at ZT 12 hr and ZT 36 hr (Fig. 3). These results suggest that RVE5
324 controls the expression of *ELF4* and other clock genes under warm temperature
325 conditions.

326 The expression of *PIF4* was increased in *rve5-2* mutant plants when
327 compared to that in WT plants at 29°C at ZT 12 hr, ZT 16 hr, ZT 36 hr, and ZT
328 40 hr (Fig. 3), which is consistent with the lower level of *ELF4* expression and
329 longer hypocotyl phenotype of *rve5-2* mutant plants at 29°C. We also checked
330 the expression of PIF4 downstream genes (Wang *et al.*, 2018), and found that
331 the transcript levels of *YUCCA 8* (*YUC8*, At4g28720), Indole-3-Acetic Acid 19
332 (*IAA19*, At3g15540), and *XYLOGLUCAN ENDOTRANSGLYCOSYLASE 7*
333 (*XTR7*, At4g14130) were higher in *rve5-2* mutant plants at 29°C compared to

that in WT plants (Fig. S4). The expression of these PIF4 downstream genes were strongly affected in the *rve5-2* mutant, suggesting that PIF4 may also subjected to RVE5-dependent post-translational modifications at warm temperature. PRR5 is known to interact with PIF4 and repress its transactivation activity (Zhu *et al.*, 2016). Indeed, the expression of *PRR5* was also affected in the *rve5-2* mutant comparing to that in the WT plants (Fig. 3). Therefore, we do not exclude the possibility that RVE5 functions through PIF4 post-translationally. It is known that EC inhibits the expression of *PIF4* (Nomoto *et al.*, 2012; Box *et al.*, 2015; Silva *et al.*, 2020), therefore, we focused on the regulation of *ELF4* expression by RVE5 at warm temperature in the later study. In addition, the phase of the expression of many of the tested clock genes was delayed (Fig. 3). Therefore, we examined activity of the circadian-regulated *CCR2::LUC* reporter in WT and *rve5-2* mutant background. Comparing to that in WT plants, delayed phase was observed in *rve5-2* mutant plants at 29°C (Fig. S5a-f), and the period of circadian clock was a little bit lengthened in *rve5-2* mutant plants, especially at 29°C (Fig. S5a-f). Taken together, these results demonstrate that RVE5 regulates the expression of clock genes such as *ELF4* under warm temperature conditions.

RVE5 has a weaker transcriptional repression activity when comparing with CCA1

As the EE *cis*-element (AAATATCT) was sown to be enriched in the binding peaks of RVE5 (Fig. 2c), to examine whether RVE5 regulates the expression of *ELF4* through the EE *cis*-element, electrophoretic mobility shift assays (EMSAs) were performed with the recombinant purified MBP-RVE5. Similar to MBP-CCA1, when MBP-RVE5 was incubated with the biotin-labelled EE identified from the promoter of *ELF4*, a band shift was observed (Fig. 4a-b), reflecting the formation of protein-DNA complexes. Adding non-labeled cold probes could compete the binding while adding the mutated form of cold probes

could not (Fig. 4a-b). This revealed the binding-specificity of RVE5 to *ELF4*-promoter DNA.

Our subcellular localization study confirmed that RVE5-YFP localizes in the nucleus (Fig. S6). To examine whether RVE5 has transcriptional activation or repressor activity, we firstly checked this in yeast cells. In contrast to the positive control, we did not observe any transcriptional activation activity associated with RVE5 (Fig. 4c). Therefore, we checked the possible transcriptional repressor activity of RVE5 in a LexA-based effector-reporter system (Lin & Little, 1989), in which a LexA fusion protein recognizes the *cis*-element presented on the LexA promoter/operator (pLexA) through the DNA-binding domain of LexA (Fig. 4d). Similar to CCA1, RVE5 had transcriptional repression activity because the LexA-RVE5 fusion protein repressed the reporter activity (Fig. 4e). Notably, RVE5 had a weaker repression activity than CCA1 (Fig. 4e). Using the promoter sequences of *ELF4* containing the EE *cis*-element (AAATATCT) in the effector-reporter assays, we confirmed that RVE5 indeed had a weaker transcriptional repression activity than CCA1 in terms of regulating the activity of *ELF4* promoter in plants (Fig. 4f-g). Therefore, RVE5 is a transcriptional repressor and has a weaker repression activity than CCA1.

RVE5 competes with CCA1 and reduces the CCA1-binding to *ELF4* promoter under warm temperature conditions

To examine how RVE5 affects the function of CCA1 in thermomorphogenesis, we expressed FLAG-tagged form of CCA1 with its native *CCA1* promoter in both WT and *rve5-2* mutant backgrounds and two independent transgenic lines with comparable CCA1-FLAG protein level in each genetic background were selected for later studies (Fig. 5a-f). Although *CCA1* expression and CCA1 protein accumulation in WT plants were low at ZT 12 hr at ambient temperature (Fig. 3 & 5a), CCA1 protein was accumulated at ZT 12 hr at warm temperatures in both genetic backgrounds (Fig. 5a-b). We performed ChIP-qPCR using

390 *CCA1:CCA1-FLAG* expressing plants grown only at 29°C at ZT 12 hr because
391 the protein level of CCA1-FLAG was low at 22°C at ZT 12 hr. The results
392 showed that CCA1-FLAG was more enriched in the promoter regions of *ELF4*
393 containing the EE *cis*-element in the *rve5-2* mutant background than that in the
394 WT background (Fig. 5g-h), which is consistent with the results that the
395 expression level of *ELF4* was lower while that of *PIF4* was higher in the
396 CCA1:*CCA1-FLAG* expressing plants in *rve5-2* mutant background than that in
397 the WT background (Fig. 6a-d)**.** We also performed ChIP-PCR at ZT 4 hr when
398 CCA1 protein abundance was higher than that at ZT 12 hr (Fig. 5a-b). The
399 results showed that the difference of CCA1-binding to *ELF4* promoter in
400 between WT and *rve5-2* mutant at ZT 4 hr was reduced than that at ZT 12 hr
401 (Fig. S7). These results demonstrate that RVE5 competes with CCA1 in binding
402 to *ELF4* promoter in the evening to regulate the expression of *ELF4* and its
403 downstream target *PIF4*.

404 LHY is partially redundant to CCA1 in terms of controlling circadian clock
405 and hypocotyl growth in Arabidopsis (Mizoguchi *et al.*, 2002). To explore the
406 genetic relationship between *RVE5* and *CCA/LHY*, we crossed *rve5-2* to *cca1-*
407 *1 lhy-20* (Marshall *et al.*, 2016) to generate the *rve5-2 cca1-1* double mutant
408 and the *rve5-2 cca1-1 lhy-20* triple mutant, and examined their hypocotyl
409 elongation phenotypes. Under ambient temperature conditions, hypocotyl
410 length of all the examined plant materials was similar (Fig. 6f-h). Under warm
411 temperature conditions, the hypocotyl length of *cca1-1* mutant was similar to
412 that of WT plants, while the hypocotyl length of *rve5-2* mutant was taller than
413 that of WT plants at warm temperatures, however, mutation of *CCA1*
414 suppressed the hypocotyl phenotype of *rve5-2* mutant (Fig. 6e & g). The
415 hypocotyl length of *cca1-1 lhy-20* double mutant plants was shorter than that of
416 WT plants, while the hypocotyl phenotype of *rve5-2* mutant was also
417 suppressed in the *rve5-2 cca1-1 lhy-20* triple mutant plants under warm

418 temperature conditions (Fig. 6f & h), suggesting that the function of *RVE5* in
419 thermomorphogenesis is partially dependent on *CCA1*/*LHY.* These results are
420 consistent with that RVE5 is competitive to CCA1 and perhaps also to LHY
421 during hypocotyl elongation under warm temperature conditions.
422 The expression level of *ELF4* transcript was decreased in *rve5-2* mutant
423 plants under warm temperature conditions (Fig. 3). To investigate whether such
424 decrease in *ELF4* gene expression contributed to the observed *rve5-2* mutant
425 phenotype. We overexpressed *ELF4* in the WT and *rve5-2* mutant backgrounds,
426 respectively, and selected two independent lines with comparable transgenic
427 expression level. Overexpression of *ELF4* in the WT background reduced
428 hypocotyl growth at 29°C, in contrast, overexpression of *ELF4* in the *rve5-2*
429 mutant background rescued the long hypocotyl phenotype of *rve5-2* mutant
430 plants at 29°C (Fig. 7a-c). EC inhibits the expression of *PIF4* (Nomoto *et al.*,
431 2012), therefore, we also checked the expression level of *PIF4* in these plant
432 materials. Agreed with the observed hypocotyl phenotypes, the expression of
433 *PIF4* was increased in *rve5-2* mutant while decreased in *ELF4* overexpression
434 plants (WT background) at 29°C, suggesting that high level of ELF4 inhibits
435 *PIF4* expression and suppresses hypocotyl elongation. In contrast, *ELF4*
436 overexpression reduced the expression level of *PIF4* in *rve5-2* mutant
437 background (Fig. 7d). We also crossed *rve5-2* mutant to *elf4-209* null mutant
438 (Kolmos *et al.*, 2009) to generate the *rve5-2 elf4-209* double mutant. The
439 hypocotyl length of *rve5-2 elf4-209* double mutant was similar to that of *elf4-*
440 *209* single mutant at both 22°C and 29°C (Fig. 7e-f), suggesting that *ELF4* is
441 epistatic to *RVE5*. The expression level of *PIF4* in *rve5-2 elf4-209* double
442 mutant was also similar to that in *elf4-209* mutant plants (Fig. 7g). Taken
443 together, these results demonstrated that *RVE5* functions upstream of *ELF4* to
444 modulate the expression level of *ELF4* and its downstream gene *PIF4* for
445 regulating hypocotyl growth at warm temperatures.

Discussion

Plants have evolved many strategies to better adapt to their given environment. For example, plants have a faster hypocotyl elongation, hyponastic leaf growth and accelerated flowering at warm temperatures (Vu *et al.*, 2019). During thermomorphogenesis, the bHLH transcription factor PIF4 is a central hub for integrating the warm temperature signals to regulate downstream gene expression involved in plant morphogenesis (Casal & Balasubramanian, 2019). Recently studies have revealed the important role of ELF3, one of the EC components, in inhibiting PIF4 protein activity both transcriptionally and post-translationally (Nomoto *et al.*, 2012; Nieto *et al.*, 2015). In the current study, we demonstrated that RVE5 regulates thermoresponsive hypocotyl growth through regulating the expression level of *ELF4*, encoding another EC component ELF4 in *Arabidopsis*, although we do not exclude the possibility that RVE5 also regulated the expression of other clock genes under warm temperature conditions.

In our working model (Fig. 8), RVE5 and CCA1 bind to the same *cis*-element presented on the promoter of *ELF4* under warm temperature conditions, but RVE5 has a weaker transcriptional repression activity than CCA1 (Fig. 4). This competition-attenuation model (Fig. 8) considers that the circadian-controlled CCA1 and LHY proteins directly suppress *ELF4* expression periodically at dawn at ambient temperature (Li *et al.*, 2011). CCA1 level is increased in response to warm temperatures in WT plants (Fig. 5a-f), however, RVE5 is also increased under warm temperature conditions (Fig. 2a) to reduce the inhibitory effect of CCA1/LHY on *ELF4* expression, therefore, the expression level of *ELF4* is maintained to a relatively high homeostatic level (Fig. 3). The encoding ELF4 protein incorporates into the EC {Herrero, 2012 #60}, which inhibits the expression of *PIF4* (Nomoto *et al.*, 2012). In the *rve5-2* mutant plants, higher

occupancy of CCA1 at the *ELF4* promoter given of the absence of RVE5 (Fig. 5g-h) Thus counter intuitively for the removal of the RVE5 repressor of *ELF4*, this results in a reduced expression of *ELF4* (Fig. 6a), which leads to elevated *PIF4* expression (Fig. 6b) and promotes taller hypocotyls under warm temperature conditions (Fig. 1a-b).

The EC activity is finely tuned at warm temperature (Zhang *et al.*, 2021b). Recently, we demonstrated that ELF3 protein level is subjected to proteolysis mediated by XBAT31/35 under warm temperature conditions (Zhang *et al.*, 2021a; Zhang *et al.*, 2021c). Functional ELF3 structures also disapate under warming conditions {Ronald, 2021 #62}, and ELF4 is known to convey thermal information {Chen, 2020 #33}. Our results here demonstrated that maintaining *ELF4* expression by RVE5 during the daytime (evening) is also important for controlling hypocotyl growth at warm temperatures in *Arabidopsis*. Since RVE5 directly binds to promoters of other clock genes and regulates the expression of many clock genes, we do not exclude the possibility that RVE5 also functions in thermomorphogenesis during the night-time period at warm temperature through other unknown mechanisms.

While CCA1 and LHY are deemed core members of the circadian clock, RVE1, RVE3 and RVE5 play a modest role in controlling clock under prevailing ambient temperature conditions (Gray *et al.*, 2017). In the current study, we found that RVE5 functions in regulating the circadian gene expression under warm-temperature conditions (Fig. 3), further the understanding of RVE5 in controlling the circadian clock at warm temperatures. Our ChIP-Seq experiment showed that many clock-related genes are also direct targets of RVE5 (Fig. 2), suggesting that RVE5 is involved in circadian clock function itself. Indeed, our circadian reporter *CCR2::LUC* experiments demonstrate that mutation of *RVE5* leads to long-period and phase delay under warm temperature conditions (Fig. S3).

CCA1 is critical in regulating thermoresponsive hypocotyl growth, as expression of *ELF4* is impaired only in *rve5-2* mutant at 29ºC (Fig. 3). The hypocotyl length of *RVE5* overexpression plants was not dramtically affected at 29ºC (Fig. S2), further suggests that CCA1 has dominant roles in this process. The protein level of CCA1 was increased (Fig, 5a) while the expression of *CCA1* decreased (Fig. 3) under warm temperature conditions. It has been hypothesized that this is because of auto-regulation of CCA1 (Wang & Tobin, 1998). CCA1 occupancy of the *ELF4* promoter was found to be increased in *rve5-2* mutant at ZT 12 hr at 29ºC (Fig. 5g-h), indicating that temperature-mediated changes in CCA1 stability is central to this control.

Protein levels of CCA1 at ZT 12 hr are decreased comparing to that at ZT 4 hr (Fig. 5a), while the protein level of RVE5 is constantly increased at 29°C (Fig. 2a). This is consistent with a specificity role of RVE5 at warm temperatures. Indeed RVE5 is the RVE most dramatically regulated by warming {Zhang, 2017 #39}. How the protein stability of RVE5 is controlled at warm temperature is currently not known. Sumoylation is a post-translational regulatory process that conjugates small ubiquitin-like modifier (SUMO) proteins to target proteins to enhance protein stability (Miura *et al.*, 2007). Sumoylation of CCA1 was previously reported (Hansen *et al.*, 2017) and RVE5 is predicted to have sumoylation sites. Therefore, it is possible that RVE5 is subjected to sumoylation at warm temperature, which awaits future investigation.

Because the *rve5-2* mutant has the long hypocotyl phenotype only at a warm temperature (Fig. 1a-b), we consider that those mis-expressed genes specifically at warm temperatures attributes to the observed hypocotyl phenotype. We do not exclude the possibility that RVE5 has additional biological functions outside of thermomorphogenesis, because there are mis-expressed clock genes in *rve5-2* mutant plants at an ambient temperature. We found a slight increase of *PIF4* expression at 22ºC but did not observe the long

hypocotyl phenotype in *rve5-2* mutant at 22ºC, which can be explained by the multiple regulations of PIF4 at post-translational levels (Zhang *et al.*, 2021b).

The underlying molecular mechanism of RVE5's function on gene expression is quite interesting. Both RVE5 and CCA1 have transcriptional repressor activity (Fig. 4), however, CCA1 inhibits while RVE5 maintains *ELF4* expression under warm temperature conditions. It was reported that LNK1 and LNK2 act as coactivators with RVE8 to promote gene expression (Rugnone *et al.*, 2013; Xie *et al.*, 2014). Here in the current study we demonstrate that RVE5 maintains gene expression through a novel mechanism. The relative weaker repression activity of RVE5 counteracts with the strong repression activity of CCA1 on the same promoter. This lifts the repression strength of downstream gene expression. LHY is partially redundant to CCA1 and shares direct targets with CCA1 (Mizoguchi *et al.*, 2002; Adams *et al.*, 2018). Among the 722 direct targets of LHY, RVE5 shares 100 target genes including *ELF4* with LHY based on our ChIP-Seq data. Therefore, it is possible that RVE5 also competes with LHY during thermomorphogenesis.

In conclusion, our results reveal the important role of RVE5 in thermomorphogenesis, and provide a unique model to explain how the transcriptional repressor RVE5 maintain gene expression during thermormophogenesis in plants; it is a more modest repressor than a direct competitor. This provides a critical insight into how the circadian clock regulates plant growth to cope with warming temperature changes.

Supplemental information

Fig. S1. Validation of *RVE5* T-DNA mutant plants.

(**a**) Schematic map of the T-DNA insertion positions in the *RVE5* gene. Coding regions, untranslated regions and introns are indicated by the black boxes,

white boxes and black lines, respectively. (**b**) Detection of *RVE5* gene expression in wild-type (WT) and *rve5-2* mutant plants by RT-qPCR using primers flanking the T-DNA insertion. The *UBQ5* gene was used as a loading control.

Fig. S2. Phenotypic analysis of *RVE5* overexpression plants.

(a-b) Thermoresponsive hypocotyl growth of wild-type (WT) plants and *RVE5-MYC* overexpression plants (*RVE5*ox-3/*RVE5*ox-8/*RVE5*ox-10). All the materials grown at 22°C were kept at 22°C or transferred to 29°C for 3 days, after which plants were imaged (a) and their hypocotyl lengths were subsequently measured (b). Error bars depict SD (n=22). Letters above the bars indicate significant differences as determined by HSD test ($P < 0.05$). Bar = 5 mm. **(c)** Validation of transgenic lines. WT and *RVE5-MYC* overexpression plants were sampled at ZT12 hr for RT-qPCR analysis of *RVE5* expression. Relative gene expression is the expression level of *RVE5* (total) normalized to that in the sample of WT at 22°C, both of which were normalized to that of *PP2A*. The bars depict the *SE* (n=3).

Fig. S3. Thermoresponsive hypocotyl growth in the dark. Wild-type (WT) plants, *RVE5* mutant (*rve5-2*), and genetic complemented plants (COM25/COM34/COM29) were grown at 22°C or 29°C in darkness for 3 days and photographed (a), and the hypocotyl length of each plant was subsequently measured (b). Error bars depict *SD* (n=24). Letters above the bars indicate significant differences as determined by HSD test ($P < 0.05$). Bar = 5 mm.

Fig. S4. Gene expression analysis of PIF4 downstream genes. Five-day-old Wild-type (WT) and *RVE5* mutant (*rve5-2*) plants grown at 22°C were maintained at 22°C or transferred to 29°C and sampled at three different time points (ZT) for quantitative gene expression analysis. The expression level of each gene was normalized to that of the WT at ZT12 hr at 22°C, which was normalized to that of *PP2A*. Data are means ± SE (n = 3).

Fig. S5. Effect of *RVE5* mutation on circadian phase and period.

(**a-f**) Circadian rhythm measurements in WT and *rve5-2* mutant plants. The circadian reporter CCR2::LUC was introduced into the WT background (WT) and rve5-2 background (rve5-2), respectively. Two independent transgenic lines (a-c and b-f) in each background were selected. Five-day-old transgenic plants grown at 22°C were kept at 22°C or transferred to 29°C for one day, and then subjected to automatic luciferase measurement (a-b, d-e). Period of clock was calculated (c & f). The bars depict the SD (n=17-19). Asterisks indicate significance levels in Student's t-tests (***P < 0.001).

Fig. S6. Subcellular localization of RVE5-YFP.

The YFP-tagged RVE5 or the empty vector alone (YFP) were transiently expressed in tobacco leaves and observed under YFP channel or bright field. Bar = 50 μm.

Fig. S7. CCA1-binding to *ELF4* promoter under warm temperature conditions.

(a) Western blotting analysis. *CCA1-FLAG* was expressed with the *CCA1* native promoter in the wild type (WT) or *rve5-2* mutant background. Transgenic plants in the WT background (CCA1-21) and *rve5-2* mutant background (CCA1-17) grown at 29°C were harvested at ZT 4 hr for western-blotting analysis. Tubulin served as a protein-loading control. Signal intensity of each band was quantified and normalized to that of the first sample. Three biological replicates (REP) are shown in the figure. **(b)** ChIP-qPCR. Plants grown at 29°C were harvested at ZT 4 hr for ChIP-qPCR using *anti*-FLAG antibody. IgG was used as a negative control. Relative enrichment of each sample was normalized to that of IgG sample at 29°C, both of which were normalized to that of the *TA3* control. Error bar represents SE (n = 3).

Table S1. Primers used in this study.

Table S2. Direct targets of RVE5 identified by ChIP-Seq.

Acknowledgements

This project was financially supported by grants from Zhejiang Provincial Talent Program (2019R52005), the Fundamental Research Funds for Zhejiang Provincial Universities (2021XZZX023), National Natural Science Foundation of China (31625004), 111 Project (B14027), and the BBSRC (BB/N018540/1).

Author contributions

J.X.L. and W.L. designed the experiments; W. L., Y.Y.T., J.Y.L. L.Y. and L.L.Z., performed the experiments; J.X.L. W.L. X.D.X. and Z.Y.W. analysed the data; J.X.L., and S.J.D wrote the paper.

Declaration of interests

The authors declare no competing interests.

References

Adams S, Grundy J, Veflingstad SR, Dyer NP, Hannah MA, Ott S, Carre IA. 2018. Circadian control of abscisic acid biosynthesis and signalling pathways revealed by genome-wide analysis of LHY binding targets. *New Phytologist* **220**(3): 893-907.

Alabadi D, Oyama T, Yanovsky MJ, Harmon FG, Mas P, Kay SA. 2001. Reciprocal regulation between TOC1 and LHY/CCA1 within the Arabidopsis circadian clock. *Science* **293**(5531): 880-883.

Box MS, Huang BE, Domijan M, Jaeger KE, Khattak AK, Yoo SJ, Sedivy EL, Jones DM, Hearn TJ, Webb AAR, et al. 2015. ELF3 controls thermoresponsive growth in Arabidopsis. *Current Biology* **25**(2): 194-199.

Casal JJ, Balasubramanian S 2019. Thermomorphogenesis. Annual Review of Plant Biology, 321-346.

Chen WW, Takahash N, Hirata Y, Ronald J, Porco S, Davis SJ, Nusinow DA, Kay SA, Mas P. 2020. A mobile ELF4 delivers circadian temperature information from shoots to roots. *Nature Plants* **6**(4): 416-426.

Clough SJ, Bent AF. 1998. Floral dip: a simplified method for Agrobacterium-mediated transformation of *Arabidopsis thaliana*. *Plant Journal* **16**(6): 735-743.

Creux N, Harmer S. 2019. Circadian rhythms in plants. *Cold Spring Harbor Perspectives in Biology* **11**(9), a034611.

Ding L, Wang S, Song ZT, Jiang Y, Han JJ, Lu SJ, Li L, Liu JX. 2018. Two B-box domain proteins, BBX18 and BBX23, interact with ELF3 and regulate thermomorphogenesis in Arabidopsis. *Cell Reports* **25**(7): 1718-1728.

Ezer D, Jung JH, Lan H, Biswas S, Gregoire L, Box MS, Charoensawan V, Cortijo S, Lai X, Stockle D, et al. 2017. The evening complex coordinates environmental and endogenous signals in Arabidopsis. *Nature Plants* **3**:17087.

Farre EM. 2012. The regulation of plant growth by the circadian clock. *Plant Biology* **14**(3): 401-410.

Fowler S, Lee K, Onouchi H, Samach A, Richardson K, Coupland G, Putterill J. 1999. GIGANTEA: a circadian clock-controlled gene that regulates photoperiodic flowering in Arabidopsis and encodes a protein with several possible membrane-spanning domains. *EMBO Journal* **18**(17): 4679-4688.

Franklin KA, Lee SH, Patel D, Kumar SV, Spartz AK, Gu C, Ye S, Yu P, Breen G, Cohen JD, et al. 2011. PHYTOCHROME-INTERACTING FACTOR 4 (PIF4) regulates auxin biosynthesis at high temperature. *Proceedings of the National Academy of Sciences of the United States of America* **108**(50): 20231-20235.

Gao J, Wang MJ, Wang JJ, Lu HP, Liu JX. bZIP17 regulates heat stress tolerance at reproductive stage in Arabidopsis. *aBIOTECH* **3**(1): 1-11.

Gray JA, Shalit-Kaneh A, Chu DN, Hsu PY, Harmer SL. 2017. The REVEILLE clock genes inhibit growth of juvenile and adult plants by control of cell size. *Plant Physiology* **173**(4): 2308-2322.

Hansen LL, Imrie L, Le Bihan T, van den Burg HA, van Ooijen G. 2017. Sumoylation of the plant clock transcription factor CCA1 suppresses DNA binding. *Journal of Biological Rhythms* **32**(6): 570-582.

Herrero E, Kolmos E, Bujdoso N, Yuan Y, Wang M, Berns MC, Uhlworm H, Coupland G, Saini R, Jaskolski M, et al. 2012. EARLY FLOWERING4 recruitment of EARLY FLOWERING3 in the nucleus sustains the Arabidopsis circadian clock. *Plant Cell* **24**(2): 428-443.

Hsu PY, Devisetty UK, Harmer SL. 2013. Accurate timekeeping is controlled by a cycling activator in Arabidopsis. *eLife* **2**, e00473.

Hsu PY, Harmer SL. 2014. Wheels within wheels: the plant circadian system. *Trends in Plant Science* **19**(4): 240-249.

Huang H, Nusinow DA. 2016. Into the Evening: complex interactions in the Arabidopsis circadian clock. *Trends in Genetics* **32**(10): 674-686.

Jung JH, Barbosa AD, Hutin S, Kumita JR, Gao M, Derwort D, Silva CS, Lai X, Pierre E, Geng F, et al. 2020. A prion-like domain in ELF3 functions as a thermosensor inArabidopsis. *Nature* **585**, 256-260.

Jung JH, Domijan M, Klose C, Biswas S, Ezer D, Gao M, Khattak AK, Box MS, Charoensawan V, Cortijo S, et al. 2016. Phytochromes function as thermosensors in Arabidopsis. *Science* **354**(6314): 886-889.

Kamioka M, Takao S, Suzuki T, Taki K, Higashiyama T, Kinoshita T, Nakamichi N. 2016. Direct repression of evening genes by CIRCADIAN CLOCK-ASSOCIATED1 in the Arabidopsis circadian clock. *Plant Cell* **28**(3): 696-711.

Koini MA, Alvey L, Allen T, Tilley CA, Harberd NP, Whitelam GC, Franklin KA. 2009. High temperature-medated adaptations in plant architecture require the bHLH transcription factor PIF4. *Current Biology* **19**(5): 408-413.

Kolmos E, Nowak M, Werner M, Fischer K, Schwarz G, Mathews S, Schoof H, Nagy F, Bujnicki JM, Davis SJ. 2009. Integrating ELF4 into the circadian system through combined structural and functional studies. *HFSP Journal* **3**(5): 350-366.

Kuno N, Moller SG, Shinomura T, Xu XM, Chua NH, Furuya M. 2003. The novel MYB protein EARLY-PHYTOCHROME-RESPONSIVE1 is a component of a slave circadian oscillator in Arabidopsis. *Plant Cell* **15**(10): 2476-2488.

Legris M, Klose C, Burgie ES, Rojas CC, Neme M, Hiltbrunner A, Wigge PA, Schafer E, Vierstra RD, Casal JJ. 2016. Phytochrome B integrates light and temperature signals in Arabidopsis. *Science* **354**(6314): 897-900.

Lesk C, Rowhani P, Ramankutty N. 2016. Influence of extreme weather disasters on global crop production. *Nature* **529**(7584): 84-87.

Li G, Siddiqui H, Teng YB, Lin RC, Wan XY, Li JG, Lau OS, Ouyang XH, Dai MQ, Wan JM, et al. 2011. Coordinated transcriptional regulation underlying the circadian clock in Arabidopsis. *Nature Cell Biology* **13**(5): 616-622.

Lin JY, Xu Y, Zhu ZQ. 2020. Emerging plant thermosensors: from RNA to protein. *Trends in Plant Science* **25**(12): 1187-1189.

Lin LL, Little JW. 1989. Autodigestion and reca-dependent cleavage of ind- mutant LexA proteins. *Journal of Molecular Biology* **210**(3): 439-452.

Marshall CM, Tartaglio V, Duarte M, Harmon FG. 2016. The Arabidopsis sickle mutant exhibits altered circadian clock responses to cool temperatures and temperature-dependent alternative splicing. *Plant Cell* **28**(10): 2560-2575.

Miura K, Jin JB, Hasegawa PM. 2007. Sumoylation, a post-translational regulatory-process in plants. *Current Opinion in Plant Biology* **10**(5): 495-502.

Mizoguchi T, Wheatley K, Hanzawa Y, Wright L, Mizoguchi M, Song HR, Carre IA, Coupland G. 2002. LHY and CCA1 are partially redundant genes required to maintain circadian rhythms in Arabidopsis. *Developmental Cell* **2**(5): 629-641.

Mizuno T, Nomoto Y, Oka H, Kitayama M, Takeuchi A, Tsubouchi M, Yamashino T. 2014. Ambient temperature signal feeds into the circadian clock transcriptional circuitry through the EC night-time repressor in *Arabidopsis thaliana*. *Plant and Cell Physiology* **55**(5): 958-976.

Nagel DH, Doherty CJ, Pruneda-Paz JL, Schmitz RJ, Ecker JR, Kay SA. 2015. Genome-wide identification of CCA1 targets uncovers an expanded clock network in Arabidopsis. *Proceedings of the National Academy of Sciences of the United States of America* **112**(34): E4802-E4810.

Nieto C, Lopez-Salmeron V, Daviere J-M, Prat S. 2015. ELF3-PIF4 interaction regulates plant growth independently of the Evening Complex. *Current Biology* **25**(2): 187-193.

Nomoto Y, Kubozono S, Yamashino T, Nakamichi N, Mizuno T. 2012. Circadian clock- and PIF4-controlled plant growth: A coincidence mechanism directly integrates a hormone signaling network into the photoperiodic control of plant architectures in Arabidopsis thaliana. *Plant and Cell Physiology* **53**(11): 1950-1964.

Nusinow DA, Helfer A, Hamilton EE, King JJ, Imaizumi T, Schultz TF, Farre EM, Kay SA. 2011. The ELF4-ELF3-LUX complex links the circadian clock to diurnal control of hypocotyl growth. *Nature* **475**(7356): 398-402.

Park YJ, Kim JY, Lee JH, Han SH, Park CM. 2021. External and internal reshaping of plant thermomorphogenesis. *Trends in Plant Science* **26**, 810-821.

Quint M, Delker C, Franklin KA, Wigge PA, Halliday KJ, van Zanten M. 2016. Molecular and genetic control of plant thermomorphogenesis. *Nature Plants* **2**(1): 15190.

Rawat R, Schwartz J, Jones MA, Sairanen I, Cheng Y, Andersson CR, Zhao Y, Ljung K, Harmer SL. 2009. REVEILLE1, a Myb-like transcription factor, integrates the circadian clock and auxin pathways. *Proceedings of the National Academy of Sciences of the United States of America* **106**(39): 16883-16888.

Rawat R, Takahashi N, Hsu PY, Jones MA, Schwartz J, Salemi MR, Phinney BS, Harmer SL. 2011. REVEILLE8 and PSEUDO-REPONSE REGULATOR5 form a negative feedback loop within the Arabidopsis circadian clock. *PLoS Genetics* **7**(3), e1001350.

Rugnone ML, Soverna AF, Sanchez SE, Schlaen RG, Hernando CE, Seymour DK, Mancini E, Chernomoretz A, Weigel D, Mac P, et al. 2013. LNK genes integrate light and clock signaling networks at the core of the Arabidopsis oscillator. *Proceedings of the National Academy of Sciences of the United States of America* **110**(29): 12120-12125.

Shalit-Kaneh A, Kumimoto RW, Filkov V, Harmer SL. 2018. Multiple feedback loops of the Arabidopsis circadian clock provide rhythmic robustness across environmental conditions. *Proceedings of the National Academy of Sciences of the United States of America* **115**(27): 7147-7152.

Silva CS, Nayak A, Lai X, Hutin S, Hugouvieux V, Jung J-H, Lopez-Vidriero I, Franco-Zorrilla JM, Panigrahi KCS, Nanao MH, et al. 2020. Molecular mechanisms of Evening Complex activity in Arabidopsis. *Proceedings of the National Academy of Sciences of the United States of America* **117**(12): 6901-6909.

Song ZT, Sun L, Lu SJ, Tian Y, Ding Y, Liu JX. 2015. Transcription factor interaction with COMPASS-like complex regulates histone H3K4 trimethylation for specific gene expression in plants. *Proceedings of the National Academy of Sciences of the United States of America* **112**(9): 2900-2905.

Sun J, Qi L, Li Y, Chu J, Li C. 2012. PIF4-mediated activation of *YUCCA8* expression integrates temperature into the auxin pathway in regulating Arabidopsis hypocotyl growth. *PLoS Genetics* **8**(3), e1002594.

Thines B, Harmon FG. 2010. Ambient temperature response establishes ELF3 as a required component of the core Arabidopsis circadian clock. *Proceedings of the National Academy of Sciences of the United States of America* **107**(7): 3257-3262.

Vu LD, Xu X, Gevaert K, Smet I. 2019. Developmental plasticity at high temperature. *Plant Physiology* **181**(2): 399-411.

Wang S, Ding L, Liu JX, Han JJ. 2018. PIF4-regulated thermo-responsive genes in Arabidopsis. *Biotechnology Bulletin* **34**(7): 57-65.

Wang ZY, Tobin EM. 1998. Constitutive expression of the *CIRCADIAN CLOCK ASSOCIATED 1* (*CCA1*) gene disrupts circadian rhythms and suppresses its own expression. *Cell* **93**(7): 1207-1217.

Xie QG, Wang P, Liu X, Yuan L, Wang LB, Zhang CG, Li Y, Xing HY, Zhi LY, Yue ZL, et al. 2014. LNK1 and LNK2 are transcriptional coactivators in the Arabidopsis circadian oscillator. *Plant Cell* **26**(7): 2843-2857.

Zhang LL, Li W, Tian YY, Davis SJ, Liu JX. 2021. The E3 ligase XBAT35 mediates thermoresponsive hypocotyl growth by targeting ELF3 for degradation in Arabidopsis. *Journal of Integrative Plant Biology* **63**, 1097-1103.

Zhang LL, Luo A, Davis SJ, Liu JX. 2021a. Timing to grow: roles of clock in thermomorphogenesis. *Trends in Plant Science* **26**(12), 1248-1257.

Zhang LL, Shao YJ, Ding L, Wang MJ, Davis SJ, Liu JX. 2021b. XBAT31 regulates thermoresponsive hypocotyl growth through mediating degradation of the thermosensor ELF3 in Arabidopsis. *Science Advances* **7**(19), eabf4427.

Zhang SS, Yang H, Ding L, Song ZT, Ma H, Chang F, Liu JX. 2017. Tissue-specific transcriptomics reveals an important role of the unfolded protein response in maintaining fertility upon heat stress in Arabidopsis. *Plant Cell* **29**(5): 1007-1023.

Zhu JY, Oh E, Wang T, Wang ZY. 2016. TOC1-PIF4 interaction mediates the circadian gating of thermoresponsive growth in Arabidopsis. *Nature Communications* **7**: 13692.

FIGURE LEGENDS

Fig. 1. RVE5 inhibits hypocotyl growth at warm temperatures and functions upstream of *PIF4* in Arabidopsis.

(a-b), Phenotypes of *RVE5* loss-of-function mutant and genetic complemented plants. Seedlings of wild-type (WT) plants, *RVE5* mutant (*rve5-2*), and genetic complemented plants (COM25/COM34/COM29) were examined for phenotypic analysis. **(c-d)**, Genetic analysis of *RVE5* and *PIF4* in thermo-responsive hypocotyl growth. The WT, *pif4-101* and *rve5-2* single mutants, and *rve5-2 pif4-101* double mutant plants were checked for phenotypes. All the materials grown at 22°C were kept at 22°C or transferred to 29°C for 4 days (a-b) or 3 days (c-d), after which plants were imaged and their hypocotyl lengths were subsequently measured. Error bars depict *SD* (n=22). Letters above the bars indicate significant differences as determined by HSD test ($P < 0.05$). Bar = 5 mm.

Fig. 2. RVE5 has overlapping genome-wide direct targets including clock-associated genes with CCA1.

(a), Accumulation of RVE5 protein level in response to warm temperature. Seven-day-old *RVE5-MYC* transgenic seedlings grown at 22°C were kept at 22°C or transferred to 29°C, after which the fusion protein was checked by western blotting with *anti*-MYC antibody. Tubulin served as a protein loading control. Signal intensity of each band was quantified and normalized to that of the first sample. **(b-d)**, ChIP-Seq analysis of RVE5-binding targets. The distribution of ChIP-Seq signals on genebody, upstream 2K and downstream 2K regions was examined (b) and the common RVE5-binding motifs among the 385 binding peaks were obtained (c-d). **(e)**, Venn diagram showing the number of overlapping binding targets between RVE5 and CCA1. **(f)**, Distribution of RVE5-binding peaks on clock-related genes in the Integrative Genomics Viewer. In the gene model, blue boxes represent exons and blue lines represent

introns, arrows indicate the direction of transcription. Reads are aligned from input (blue) and ChIP (red) with three replicates. Binding to the promoter of *ELF3*, *PRR9*, *CCA1*, *LHY*, or *PIF4* was not significant (P<0.05). **(g-i)**, *in vivo* binding of RVE5 to the promoters of *ELF4*, *PRR5* and *PRR7* under two temperature conditions. Transgenic plants overexpressing *RVE5-MYC* grown at 22°C or 29°C for 12 hr or 36 hr were harvested and ChIP-qPCR was performed using *anti*-MYC antibody. Relative enrichment of each sample was normalized to that *anti*-GST sample (IgG control) in 12 hr at 22°C, both of which were normalized to that of the *TA3* control. Error bar represents SE (n = 3). Letters above the bars indicate significant differences as determined by HSD test (P < 0.05).

Fig. 3. RVE5 regulates the expression of clock-associated genes under warm temperature conditions.

Five-day-old WT plants as well as *RVE5* mutant (*rve5-2*) plants grown at 22°C were kept at 22°C or transferred to 29°C, after which total seedlings were sampled at different ZT times as indicated for RT-qPCR analysis. Relative gene expression is the expression level of each gene normalized to that of *PP2A*. The bars depict the *SE* (n=3).

Fig. 4. RVE5 has a weaker transcriptional repression activity than CCA1.

(a-b), Direct binding of RVE5 or CCA1 to the *ELF4* promoter sequence. MBP-tagged RVE5 (a) or CCA1 (b) was incubated with the biotin-labelled *ELF4* promoter DNA (5'-AAATATCT-3'). Non-labelled native (competitor) or mutated (5'-AAATCGAG-3') cold probes [competitor (m)] were used in the competing assays. **(c)**, Transcriptional activation activity assay in yeast cells. RVE5 was fused to the yeast GAL4 DNA-binding domain (BD). Activation of the His and Ade reporter genes in yeast cells was used for the activation assay. CONSTANS (CO) was used as a positive control. **(d-g)**, Transcriptional repression activity assay in effector-reporter assays. Schematic design for the

assay is shown in d. LexA-RVE5 or LexA-CCA1 (e), or RVE5 and CCA1 (f-g) driven by the CaMV 35S promoter was expressed as the effector, and the CaMV 35S constitutive promoter linked with a promoter-specific sequence of either pLexA or pELF4 to the firefly luciferase was used as a reporter. Renilla luciferase driven by the CaMV 35S promoter was used as an internal control. Relative luciferase activity is the firefly luciferase activity normalized to the Renilla luciferase activity, which was then normalized to the empty vector control. Western blots showing the expression level of the effector (RVE5-MYC/CCA1-MYC) in the effector-reporter assays in tobacco leaves (g). RbcS serves as a loading control. Error bars depict *SE* (n=5 in e, n=7 in f). Letters above the bars indicate significant differences as determined by HSD test ($P < 0.05$).

Fig. 5. RVE5 competes with CCA1 in DNA-binding under warm temperature conditions.

(a-d), Accumulation of CCA1 protein at warm temperatures. *CCA1-FLAG* was expressed with the *CCA1* native promoter in the wild-type (WT) or *rve5-2* mutant background. The fusion protein in the WT background (CCA1-21, a) and *rve5-2* mutant background (CCA1-17, b) were checked with *anti*-FLAG antibody at different time under two temperature conditions. Tubulin served as a protein loading control. Signal intensity of each band was quantified and normalized to that of the first sample (a-b). Two sets of independent lines with comparable expression level in WT (CCA1-21/26) and *rve5-2* mutant (CCA1-17/13) backgrounds were selected, and the fusion proteins were checked in the same blot by Western blotting at ZT 12 hr (c-d). Three independent blots were run and quantified for each set of comparison (c-d). **(e-f)**, Direct binding of CCA1 to the *ELF4* promoter in WT and *rve5-2* mutant plants. Transgenic plants expressing *CCA1-FLAG* in WT background and *rve5-2* mutant background grown at 29°C were harvested at ZT 12 hr for ChIP-qPCR using *anti*-FLAG

889 antibody. IgG was used as a negative control. Relative enrichment of each
890 sample was normalized to that of IgG sample at 29°C, both of which were
891 normalized to that of the *TA3* control. Error bar represents SE (n = 3).

892 **Fig. 6. RVE5 and CCA1/LHY have competitive roles in thermoresponsive**
893 **hypocotyl regulation.**

894 **(a-d)**, Regulation of *ELF4* and *PIF4* expression in *CCA1-FLAG* expressing
895 plants in the wild-type (WT) or *rve5-2* mutant background driven by the *CCA1*
896 native promoter at ZT 36 hr. Relative gene expression is the expression level
897 of *ELF4* or *PIF4* normalized to that of *PP2A*. The bars depict the *SE* (n=3). **(e-**
898 **h)**, Genetic analysis of *RVE5* and *CCA1*/*LHY* in thermomorphogenesis. The
899 WT, *rve5-2*, *cca1-1*, *rve5-2 cca1-1*, *rve5-2 lhy-20*, and *rve5-2 cca1-1 lhy-20*
900 plants were phenotyped. Error bars depict *SD* (n=30). Letters above the bars
901 indicate significant differences as determined by HSD test ($P < 0.05$); Bar = 5
902 mm.

903 **Fig. 7. Overexpresssion of *ELF4* rescues the thermoresponsive hypocotyl**
904 **phenotype of *rve5-2* mutant plants.**

905 **(a-d)**, Suppression of *rve5-2* mutant phenotype under warm temperature
906 conditions by overexpression of *ELF4*. *ELF4* was overexpressed in the WT
907 (ELF4ox) and *rve5-2* mutant (*rve5-2* ELF4ox) background and two independent
908 transgenic lines in each background with similar transgene expression levels
909 selected and phenotyped (a-b). The expression of total *ELF4* and *PIF4* was
910 checked by RT-qPCR at ZT 36 hr (c-d). Relative gene expression is the
911 expression level in each sample normalized to that of *PP2A*. The bars depict
912 the SE (n=3). **(e-g)**, Genetic analysis between *RVE5* and *ELF4*. The *rve5-2*
913 single mutant and *elf4-209* single mutant were crossed to generate the double
914 mutant *rve5-2 elf4-209*, and the single and double mutants were phenotyped
915 (e-f). The expression of *PIF4* was checked by RT-qPCR (g). All the materials
916 grown at 22°C were kept at 22°C or transferred to 29°C for 4 days, after which

plants were imaged and their hypocotyl lengths were subsequently measured. Error bars depict SD (n=30). Letters above the bars indicate significant differences as determined by HSD test ($P < 0.05$). Bar = 5 mm.

Fig. 8. A competition-attenuation working model for modulating *ELF4* expression and thermoresponsive hypocotyl growth.

In WT plants, both RVE5 and CCA1 are transcriptional repressors and bind to the same *cis*-element presented on *ELF4* promoter. CCA1 has a stronger (S) while RVE5 has a weaker (W) transcriptional repression activity. Therefore, RVE5 attenuates the repression effect of CCA1 through competing with CCA1 in DNA binding and maintains the expression of downstream genes including *ELF4* at warm temperatures. The encoded ELF4 is assembled into an evening complex (EC) together with ELF3 and LUX to inhibit the expression of *PIF4*, a central regulator of thermomorphogenesis. In *rve5-2* mutant plants, due to the absence of RVE5, more CCA1 binds to the *ELF4* promoter and results in more inhibition of *ELF4* expression, leading to more *PIF4* expression, and subsequent more hypocotyl growth under warm temperature conditions.

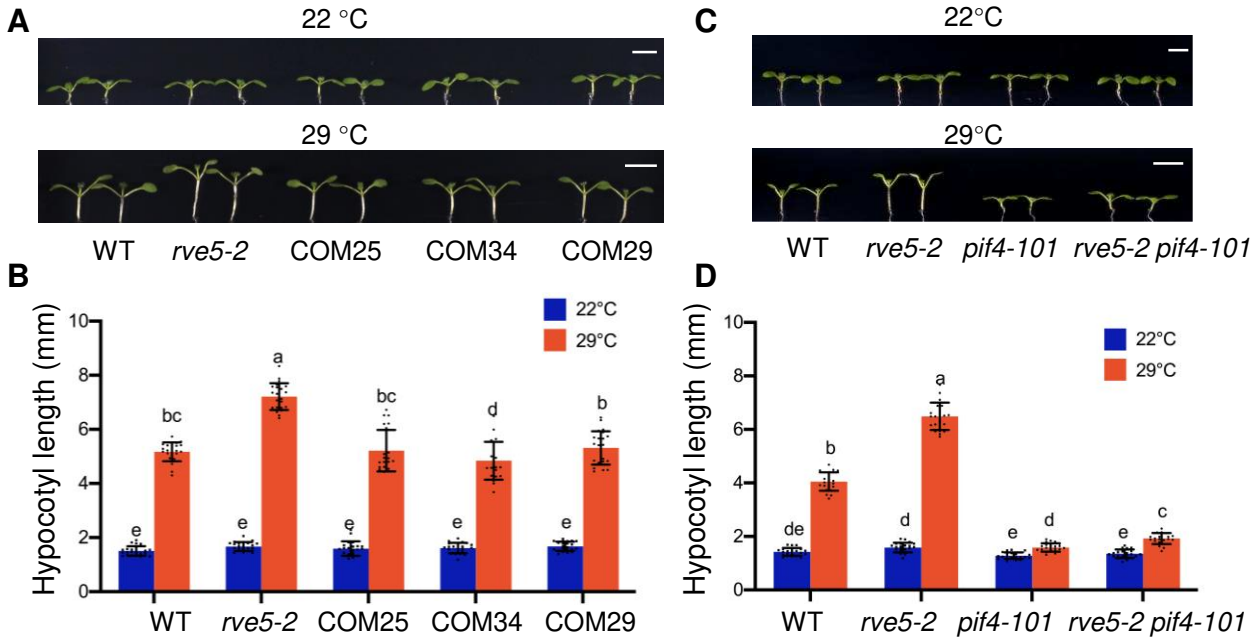

Figure 1. RVE5 Inhibits Hypocotyl Growth at Warm Temperatures and Functions Upstream of *PIF4* in Arabidopsis.
A-B, Phenotypes of *RVE5* loss-of-function mutant and genetic complemented plants. Seedlings of wild-type (WT) plants, *RVE5* mutant (*rve5-2*), and genetic complemented plants (COM25/COM34/COM29) were examined for phenotypic analysis. **C-D**, Genetic analysis of *RVE5* and *PIF4* in thermo-responsive hypocotyl growth. The WT, *pif4-101* and *rve5-2* single mutants, and *rve5-2 pif4-101* double mutant plants were checked for phenotypes. All the materials grown at 22° C were kept at 22° C or transferred to 29° C for 4 days, after which plants were imaged and their hypocotyl lengths were subsequently measured. Error bars depict *SD* (n=22). Letters above the bars indicate significant differences as determined by HSD test ($P < 0.05$). Bar = 5 mm.

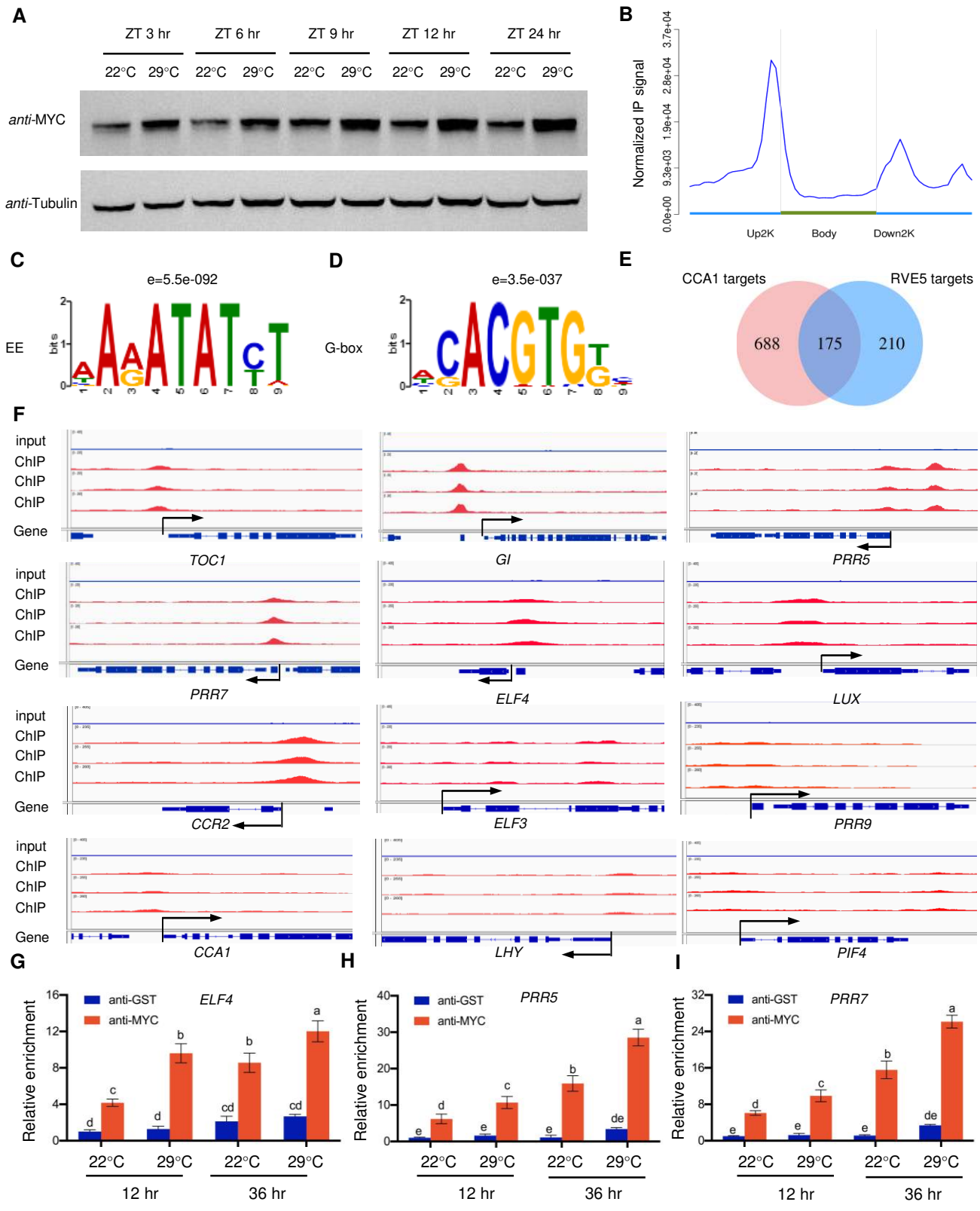

Figure 2. RVE5 Has Overlapping Genome-Wide Direct Targets including Clock-Associated Genes with CCA1.
A, Accumulation of RVE5 protein level in response to warm temperature. Seven-day-old *RVE5-MYC* transgenic seedlings grown at 22° C were kept at 22° C or transferred to 29° C, after which the fusion protein was checked by western blotting with *anti*-MYC antibody. Tubulin served as a protein loading control. **B-D**, ChIP-Seq analysis of RVE5-binding targets. The distribution of ChIP-Seq signals on genebody, upstream 2K and downstream 2K regions was examined (B) and the common RVE5-binding motifs among the 385 binding peaks were obtained (C-D). **E**, Venn diagram showing the number of overlapping binding targets between RVE5 and CCA1. **F**, Distribution of RVE5-binding peaks on clock-related genes in the Integrative Genomics Viewer. In the gene model, blue boxes represent exons and blue lines represent introns, arrows indicate the direction of transcription. Reads are aligned from input (blue) and ChIP (red) with three replicates. Binding to the promoter of *ELF3*, *PRR9*, *CCA1*, *LHY*, or *PIF4* was not significant (P<0.05). **G-I**, *in vivo* binding of RVE5 to the promoters of *ELF4*, *PRR5* and *PRR7* under two temperature conditions. Transgenic plants overexpressing *RVE5-MYC* grown at 22° C or 29° C for 12 hr or 36 hr were harvested and ChIP-qPCR was performed using anti-MYC antibody. Relative enrichment of each sample was normalized to that anti-GST sample (IgG control) in 12 hr at 22° C, both of which were normalized to that of the *TA3* control. Error bar represents SE (n = 3). Letters above the bars indicate significant differences as determined by HSD test (P < 0.05).

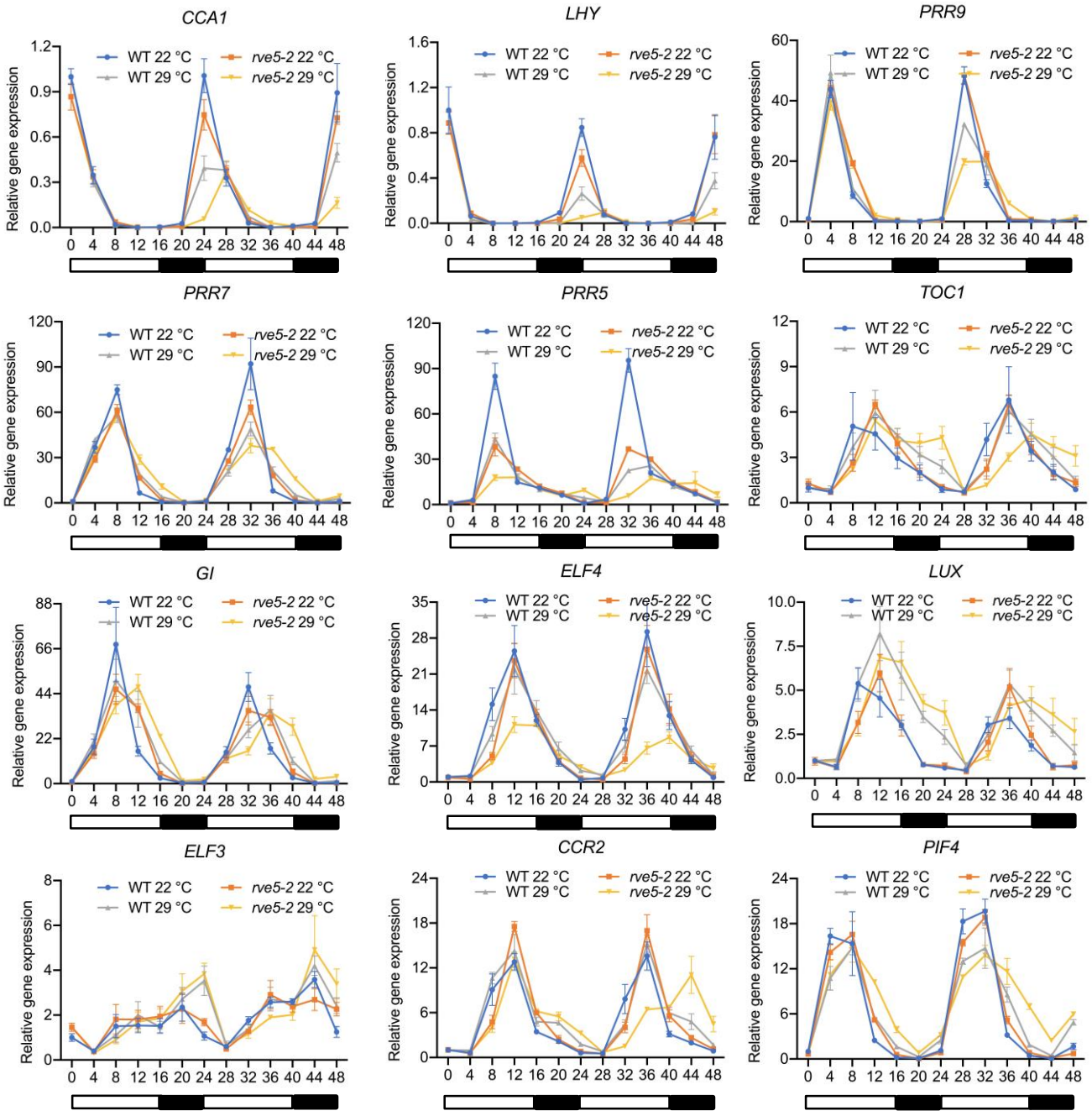

Figure 3. RVE5 Regulates the Expression of Clock-Associated Genes under Warm Temperature Conditions.
Expression of clock-associated genes in WT and *rve5-2* mutant plants under warm temperature conditions. Five-day-old WT plants as well as *RVE5* mutant (*rve5-2*) plants grown at 22° C were kept at 22° C or transferred to 29° C, after which total seedlings were sampled at different ZT times as indicated for RT-qPCR analysis. Relative gene expression is the expression level of each gene normalized to that of *PP2A*. The bars depict the *SE* (n=3).

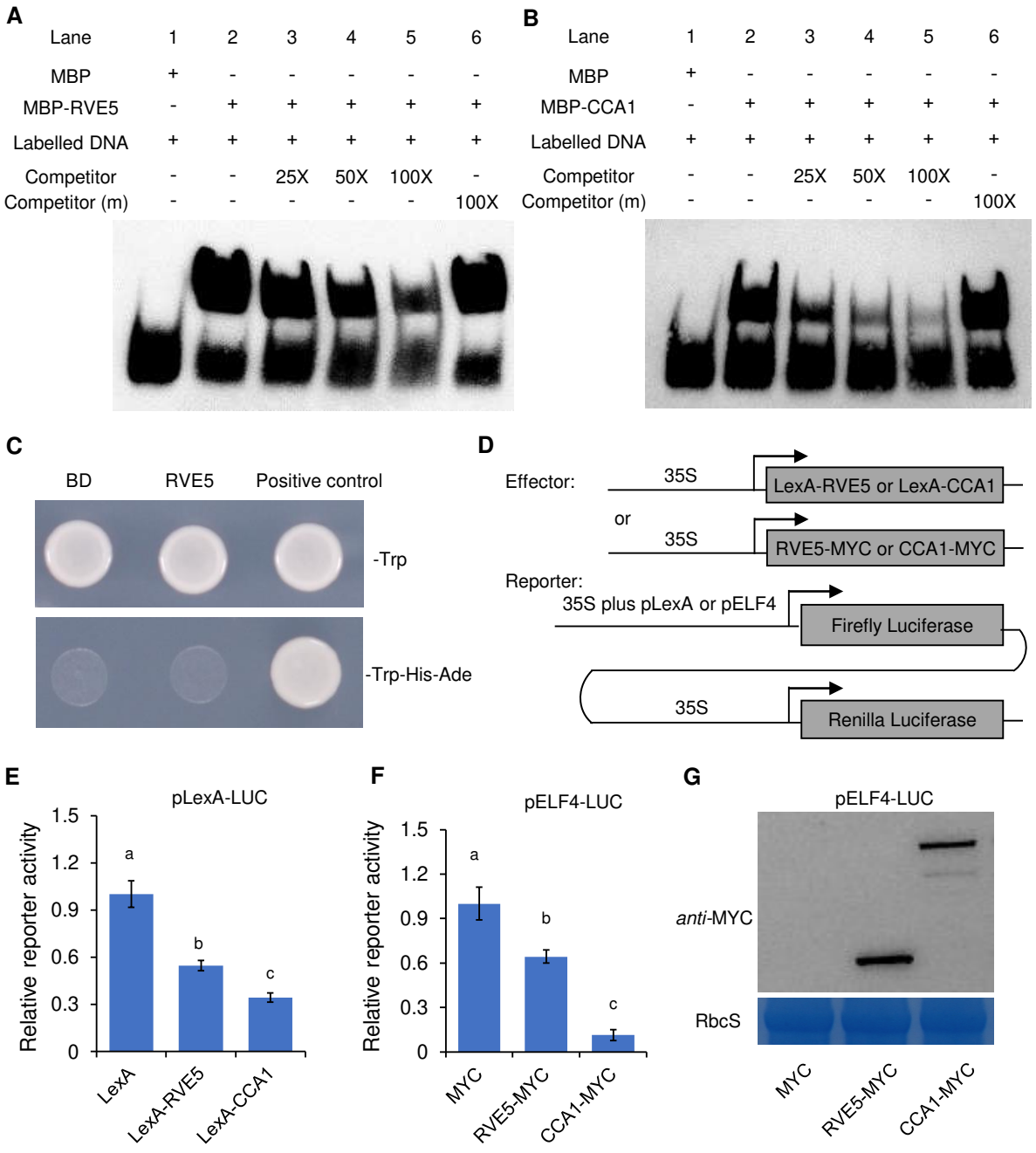

Figure 4. RVE5 Has a Weaker Transcriptional Repression Activity than CCA1.
A-B, Direct binding of RVE5 or CCA1 to the *ELF4* promoter sequence. MBP-tagged RVE5 (A) or CCA1 (B) was incubated with the biotin-labelled *ELF4* promoter DNA. Non-labelled cold probes (native or mutated competitor) were used in the competing assays. **C**, Transcriptional activation activity assay in yeast cells. RVE5 was fused to the yeast GAL4 DNA-binding domain (BD). Activation of the His and Ade reporter genes in yeast cells was used for the activation assay. CONSTANS (CO) was used as a positive control. **D-G**, Transcriptional repression activity assay in effector-reporter assays. Schematic design for the assay is shown in D. LexA-RVE5 or LexA-CCA1 (F), or RVE5 and CCA1 (G) driven by the CaMV 35S promoter was expressed as the effector, and the CaMV 35S constitutive promoter linked with a promoter-specific sequence of either pLexA or pELF4 to the firefly luciferase was used as a reporter. Renilla luciferase driven by the CaMV 35S promoter was used as an internal control. Relative luciferase activity is the firefly luciferase activity normalized to the Renilla luciferase activity, which was then normalized to the empty vector control. Western blots showing the expression level of the effector (RVE5-MYC/CCA1-MYC) in the effector-reporter assays in tobacco leaves (G). RbcS serves as a loading control. Error bars depict *SE* (n=5 in e, n=7 in f). Letters above the bars indicate significant differences as determined by HSD test ($P < 0.05$).

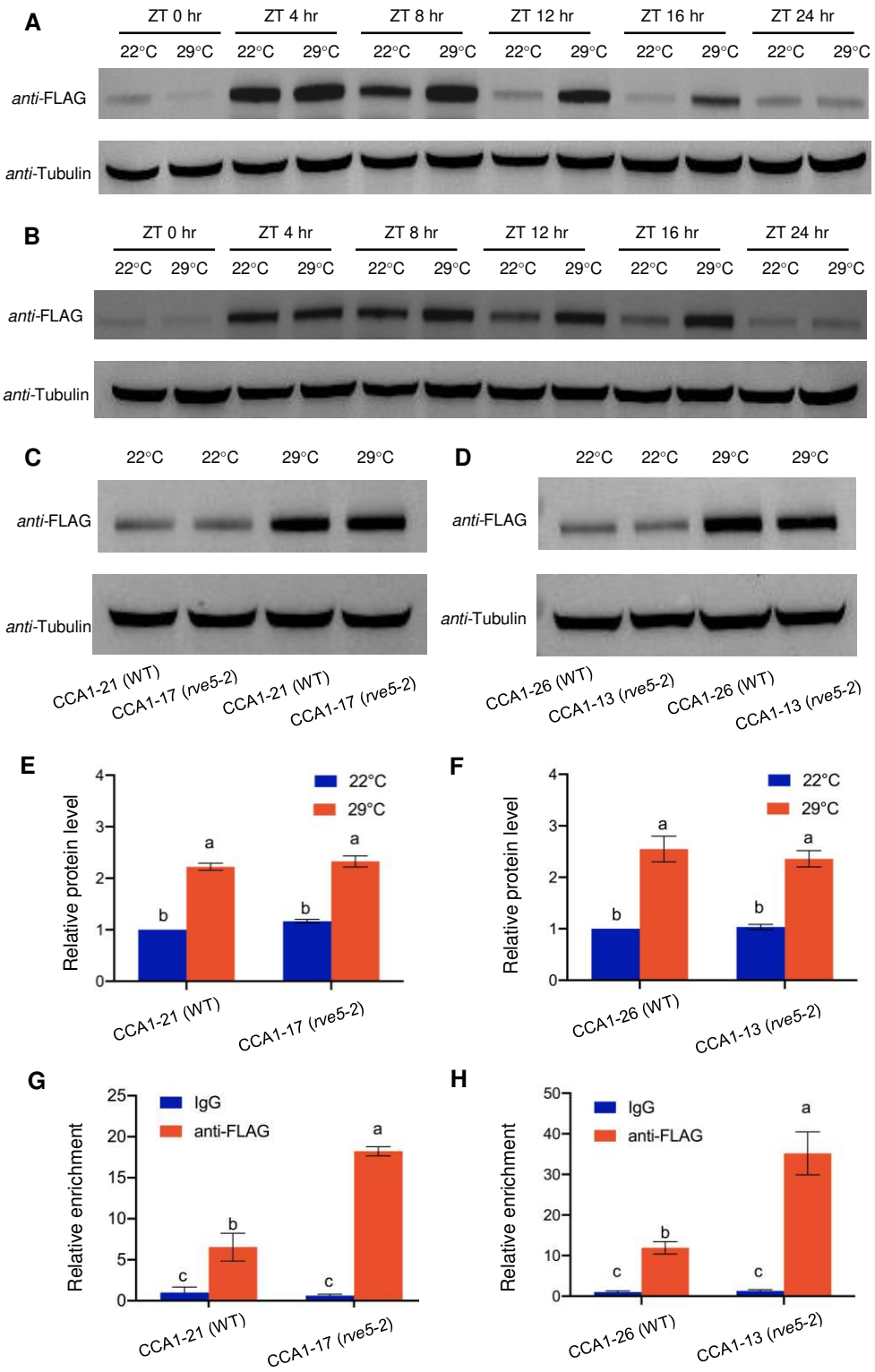

Figure 5. RVE5 Competes with CCA1 in DNA-Binding under Warm Temperature Conditions.
A-F, Accumulation of CCA1 protein at warm temperatures. *CCA1-FLAG* was expressed with the *CCA1* native promoter in the wild-type (WT) or *rve5-2* mutant background. The fusion protein in the WT background (CCA1-21) and *rve5-2* mutant background (CCA1-17) were checked with *anti*-FLAG antibody at different time under two temperature conditions (A-B). Two independent lines with comparable expression level in WT and backgrounds were selected, and the fusion protein was checked at ZT 12 hr (C-F). Tubulin served as a protein loading control. Three independent blots were quantified. **G-H**, Direct binding of CCA1 to the *ELF4* promoter in WT and *rve5-2* mutant plants. Transgenic plants expressing *CCA1-FLAG* in WT background and *rve5-2* mutant background grown at 29° C were harvested at ZT 12 hr for ChIP-qPCR using *anti*-FLAG antibody. IgG was used as a negative control. Relative enrichment of each sample was normalized to that of IgG sample at 29° C, both of which were normalized to that of the *TA3* control. Error bar represents SE (n = 3).

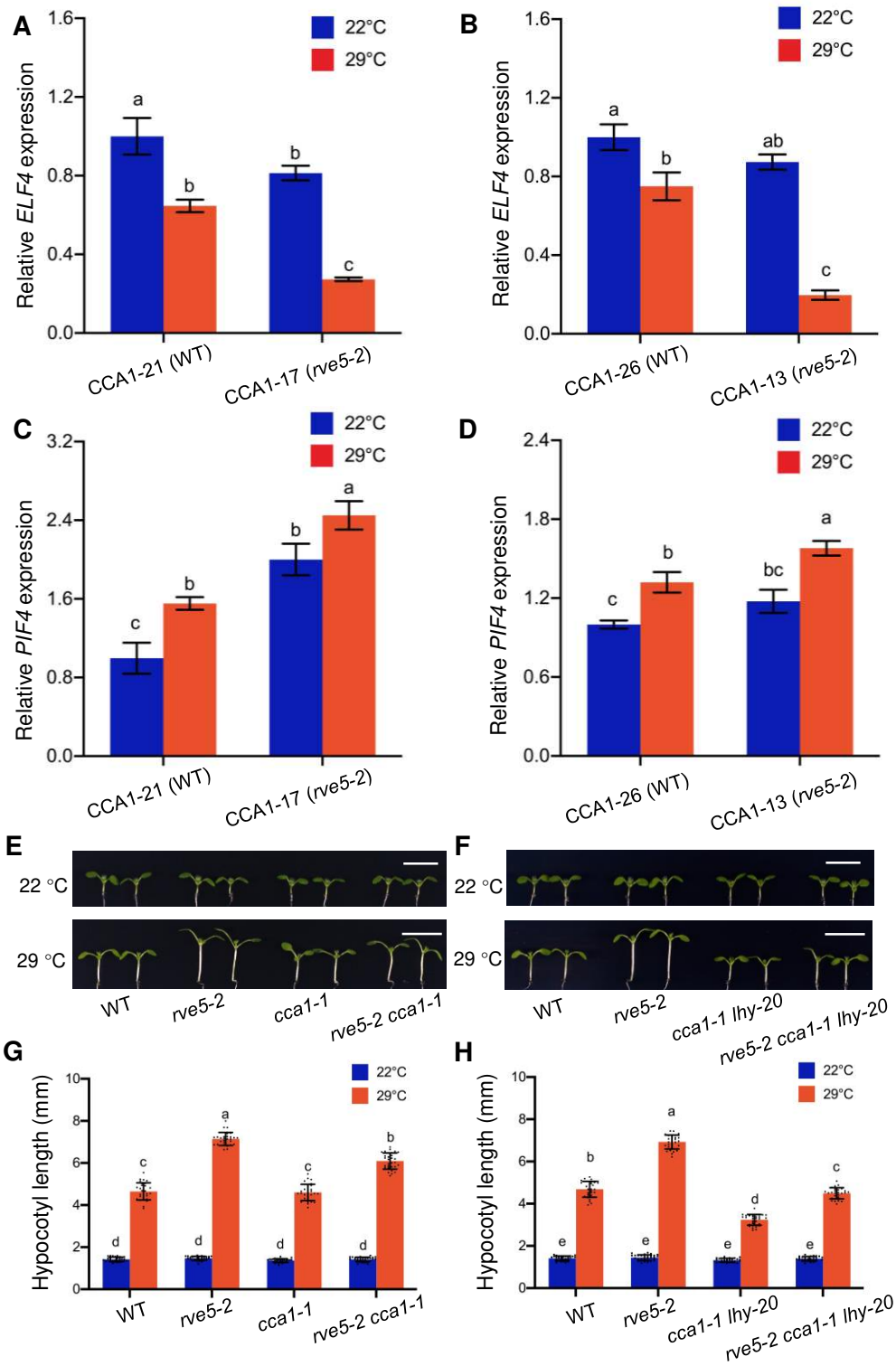

Figure 6. RVE5 and CCA1/LHY Have Competitive Roles in Thermoresponsive Hypocotyl Regulation.
A-D, Regulation of *ELF4* and *PIF4* expression in *CCA1-FLAG* expressing plants in the wild-type (WT) or *rve5-2* mutant background driven by the *CCA1* native promoter at ZT 36 hr. Relative gene expression is the expression level of *ELF4* or *PIF4* normalized to that of *PP2A*. The bars depict the *SE* (n=3). **E-H**, Genetic analysis of *RVE5* and *CCA1/LHY* in thermomorphogenesis. The WT, *rve5-2*, *cca1-1*, *rve5-2 cca1-1*, *rve5-2 lhy-20*, and *rve5-2 cca1-1 lhy-20* plants were phenotyped. Error bars depict *SD* (n=30). Letters above the bars indicate significant differences as determined by HSD test ($P < 0.05$); Bar = 5 mm.

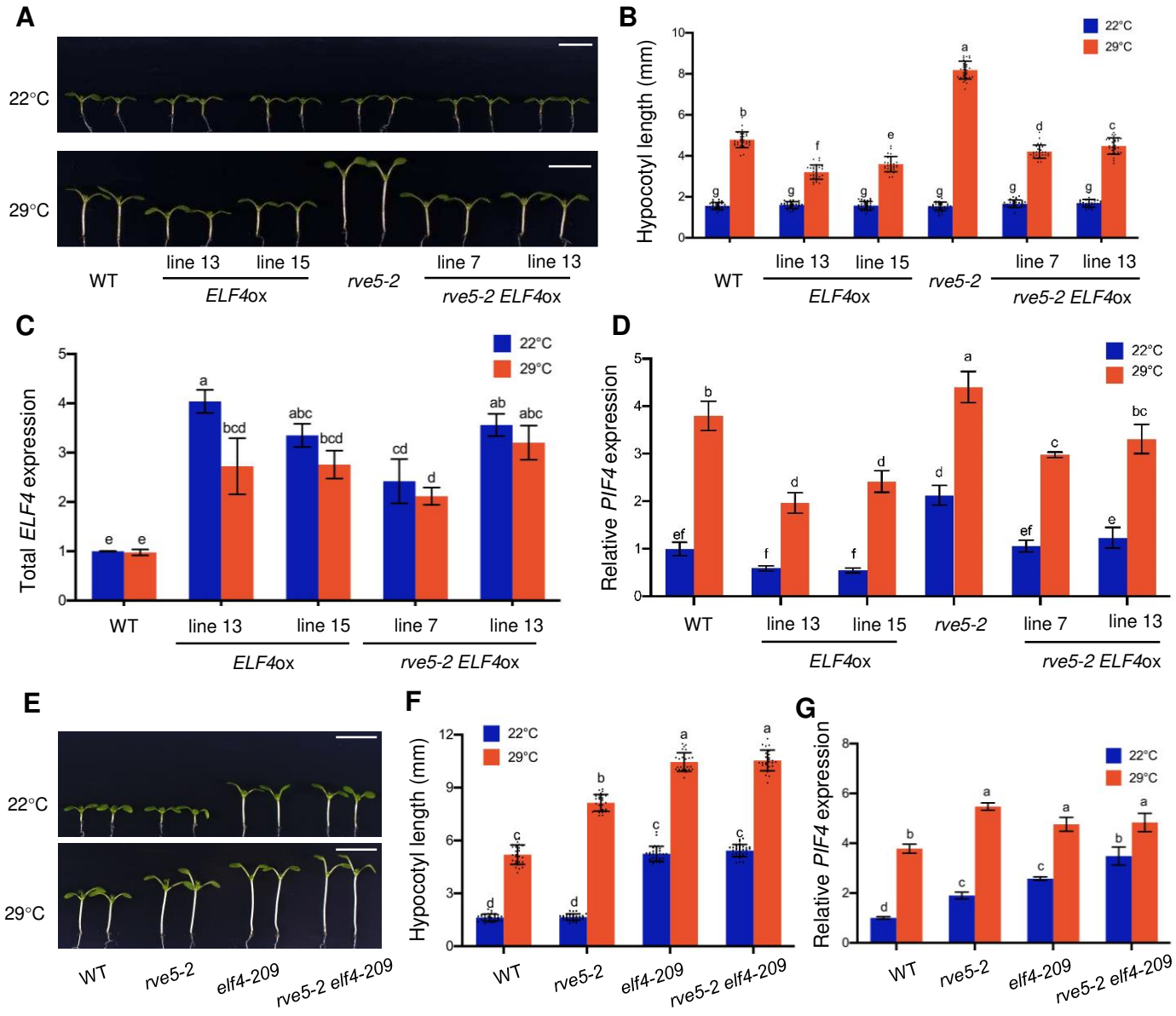

Figure 7. Overexpresssion of *ELF4* Rescues the Thermoresponsive Hypocotyl Phenotype of *rve5-2* Mutant Plants.
A-D, Suppression of *rve5-2* mutant phenotype under warm temperature conditions by overexpression of *ELF4*. *ELF4* was overexpressed in the WT (ELF4ox) and *rve5-2* mutant (*rve5-2* ELF4ox) background and two independent transgenic lines in each background with similar transgene expression levels selected and phenotyped (A-B). The expression of total *ELF4* and *PIF4* was checked by RT-qPCR at ZT 36 hr (C-D). Relative gene expression is the expression level in each sample normalized to that of *PP2A*. The bars depict the SE (n=3). **E-G**, Genetic analysis between *RVE5* and *ELF4*. The *rve5-2* single mutant and *elf4-209* single mutant were crossed to generate the double mutant *rve5-2 elf4-209*, and the single and double mutants were phenotyped (E-F). The expression of *PIF4* was checked by RT-qPCR (G). All the materials grown at 22° C were kept at 22° C or transferred to 29° C for 4 days, after which plants were imaged and their hypocotyl lengths were subsequently measured. Error bars depict SD (n=30). Letters above the bars indicate significant differences as determined by HSD test ($P < 0.05$). Bar = 5 mm.

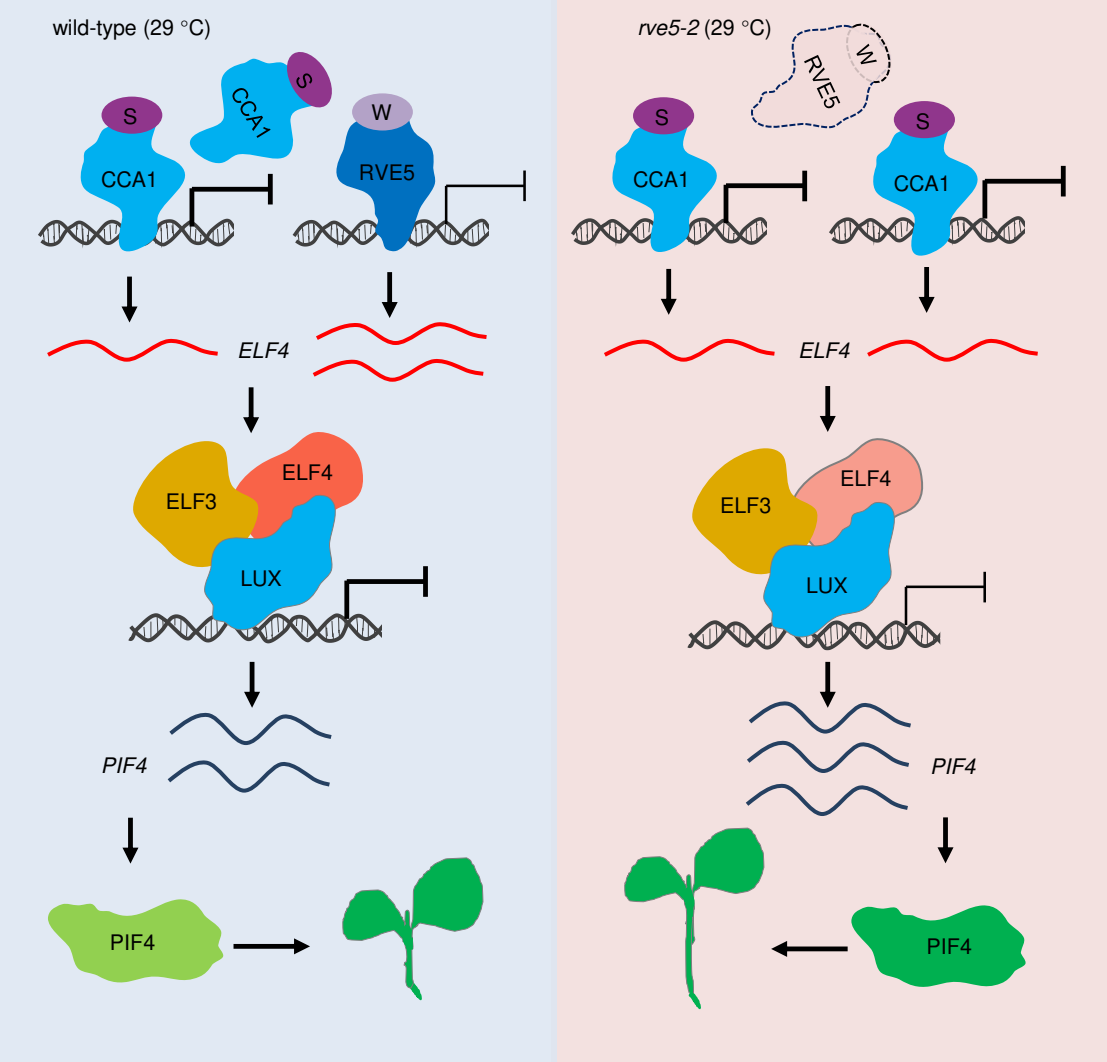

Figure 8. A competition-attenuation working model for modulating *ELF4* expression and thermoresponsive hypocotyl growth.
In WT plants, both RVE5 and CCA1 are transcriptional repressors and bind to the same *cis*-element presented on *ELF4*. CCA1 has a stronger (S) while RVE5 has a weaker (W) transcriptional repression activity. Therefore, RVE5 attenuates the repression effect of CCA1 through competing with CCA1 in DNA binding and maintains the expression of downstream genes including *ELF4* at warm temperatures. The encoded ELF4 is assembled into an evening complex (EC) together with ELF3 and LUX to inhibit the expression of *PIF4*, a central regulator of thermomorphogenesis. In *rve5-2* mutant plants, due to the absence of RVE5, more CCA1 binds to the *ELF4* promoter and results in more inhibition of *ELF4* expression, leading to disinhibition and more *PIF4* expression, and subsequent more hypocotyl growth under warm temperature conditions.